ELSEVIER

Mechanics of Materials 33 (2001) 105–120

MECHANICS OF MATERIALS

www.elsevier.com/locate/mechmat

Effect of substrate modulus difference on dislocation formation in an epitaxial film

Shing-Dar Wang [a], Sanboh Lee [b,*], Chun-Hway Hsueh [c]

[a] *Department of Mechanical Engineering, Chung Chou Junior College of Technology and Commerce, Chang-Hua, Taiwan, ROC*

[b] *Department of Materials Science and Engineering, National Tsing Hua University, 101, Sec. 2, Kuang Fu Road, Hsinchu 30013, Taiwan, ROC*

[c] *Metals and Ceramics Division, Oak Ridge National Laboratory, Oak Ridge, TN 37831-6068, USA*

Received 7 October 1999; received in revised form 2 February 2000

Abstract

The effect of substrate modulus difference on dislocation formation in an epitaxial film is derived in the present study. The analysis is based on the energy approach, in which the self-energy of the dislocation and the interaction energy between the dislocation and the mismatch strain are calculated. The elastic stress field due to the interface dislocation is derived by superposition of the elastic stress fields of the film/substrate system with the following two configurations: (i) a dislocation at the interface assuming the film is also semi-infinite, and (ii) prescribed traction on the film surface which are the negative of those calculated from the first configuration at the location equivalent to the film surface in the second configuration. The results show that the critical film thickness for forming interface dislocation increases with the decrease in the shear modulus ratio of the film to the substrate. © 2001 Elsevier Science Ltd. All rights reserved.

Keywords: Epitaxial film; Substrate; Dislocation; Critical thickness

1. Introduction

The performance of many electronic devices and high temperature superconducting films depends on the quality of crystalline films grown epitaxially on substrates of different crystals. Because of the difference in lattice parameter between the film and the substrate, the lattice mismatch exists at the film/substrate interface which, in turn, induces internal stresses in the system. These internal stresses could be relaxed by the formation of misfit dislocations at the interface (Frank and van der Merwe, 1949; Freund, 1990, 1993; Freund and Nix, 1996; Gosling and Willis, 1994; Mattews and Blakeslee, 1974; Willis et al., 1990, 1991; Zhang, 1996; Zhang et al., 1999). However, the interface dislocations inevitably degrade the device performance. Hence, the study of the condition for the interface dislocation to form in the epitaxial film/substrate system becomes crucial in the materials design. Due to the complexity of the problem, the early analyses assumed that the film and the substrate are isotropic elastic materials and have the same elastic constants. Matthews and Blakeslee (MB) (1974) considered a thin epitaxial film on an semi-infinitely thick

* Corresponding author. Tel.: +886-35-719-677; fax: +886-35-722-366.
E-mail address: sblee@mse.nthu.edu.tw (S. Lee).

0167-6636/01/$ - see front matter © 2001 Elsevier Science Ltd. All rights reserved.
PII: S 0 1 6 7 - 6 6 3 6 (0 0) 0 0 0 5 8 - 2

substrate, analyzed the force exerted by the mismatch strain and the approximate tension in the dislocation line, and used the force approach to predict the critical thickness of the film for the interface dislocation to form. The MB model was subsequently improved by others using the energy approach, in which the work of forming the dislocation due to the presence of internal stresses and the self-energy of the dislocation were analyzed. Recently, the MB criterion for a film on an semi-infinitely thick substrate was generalized by Freund and Nix (FN) (1996) using the energy approach to the case of a film deposited on a substrate with a finite thickness. Because of the complexity of the interaction between the interface dislocation and the two free surfaces, a first-order approximation was used in analyzing the self-energy of the dislocation and the free-surface condition was not satisfied in the FN model. The FN model was further improved by Zhang et al. (1999) using the superposition principle and Fourier transformation to derive a complete analysis for the dislocation self-energy and to satisfy the free-surface condition.

The analyses described above assumed the film and the substrate having the same isotropic elastic constants in order to simplify the analysis. Considering the difference in elastic constants between the film and the substrate or the elastic anisotropy of the constituents, the analyses have also been performed using Fourier transformation; however, the solutions were approximate. For example, the stress field and energy arising from an array of dislocations (Willis et al., 1991) and dislocation dipoles (Gosling and Willis, 1994) distributed uniformly on the perfectly bonded interface between an epitaxial film and a semi-infinite substrate of different isotropic elastic constants were derived. Gosling and Willis (1994) analyzed the energy of arrays of dislocations located periodically at the perfectly bonded interface between an epitaxial film and a semi-infinite substrate of the same anisotropic elastic constants. It is noted that the core energy was not included in the above analyses (Willis et al., 1991; Gosling and Willis, 1994). Including the core energy, the critical thickness of an epitaxial film on a semi-infinite substrate of different isotropic elastic constants was analyzed by Zhang (1995). However, it is noted that the displacement and the shear stress used in deriving the core energy in Zhang's analysis (Zhang, 1995) did not satisfy the continuity condition at the interface.

The purpose of the present study is to refine Zhang's analysis (Zhang, 1995) of the epitaxial film deposited on a semi-infinite substrate with different isotropic elastic constants to satisfy the continuity condition at the interface. To achieve this, the stress field due to the interface dislocation was derived by superposition of (1) the stress due to two semi-infinite medium and (2) the stress due to the prescribed traction on the film surface which were the negative of those calculated from the first component at film surface. This stress field satisfies the free-surface condition and the stress continuity condition at the film/substrate interface. Then, the predicted stress fields due to an edge and a screw dislocations are presented, respectively. Also, the critical film thickness for the interface dislocation to form is predicted and compared with existing solutions. Finally, it is noted that depending on the temperature and friction force, the dislocation will move from the hard medium to soft medium through the interface (Gutkin and Romanov, 1992) after it nucleates in the hard medium or at the interface. However, it is beyond the scope of the present study.

2. Analysis

The present model considers a film of thickness h deposited epitaxially on a semi-infinite substrate as shown in Fig. 1. Both shear modulus and Poisson's ratio of the film and the substrate are μ_f, ν_f and μ_s, ν_s, respectively. The Cartesian coordinates, x_1, x_2, and x_3 are used with the x_1-axis parallel to the in-plane interface, the x_2-axis perpendicular to the interface and the origin located at the interface. A dislocation with a Burgers vector $\mathbf{b} = [b_1, b_2, b_3]$ is located at the origin. In the following analyses, the energies are calculated per unit length of the dislocation line or per unit depth of the film/substrate system. The formation energy, E_f, of the dislocation consists of two components: E_s, the self-energy of the dislocation and E_{int}, the interaction energy between the dislocation and mismatch strain, such that

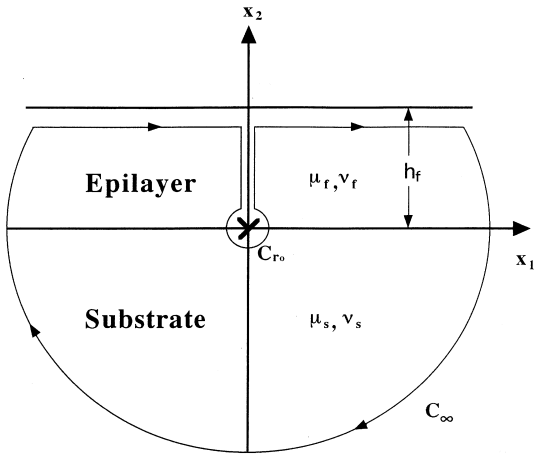

Fig. 1. A dislocation located at the perfectly bonded interface between an epilayer of thickness h and a semi-infinite substrate.

$$E_{\mathrm{f}} = E_{\mathrm{s}} + E_{\mathrm{int}}. \tag{1}$$

The energy components, E_{s} and E_{int}, can be obtained by converting an area integral (with unit depth) to a line integral using a divergence theory. Since the elastic stress field induced by a dislocation is not valid in the core region, the integration path for E_{s} is selected as two contours C_{r_0} and C_∞ and an arbitrary cut (see Fig. 1) where r_0 is the core radius of the dislocation. Accordingly, the self-energy of the dislocation, E_{s}, can be decomposed into two components: E_{c}, the integration along the core contour C_{r_0} (i.e., the dislocation core energy), and E_0, the difference between the self-energy and the core energy. For convenience, the arbitrary cut is usually made along the x_2-axis. Using the traction-free condition along the surface, $x_2 = h$, and the vanishing remote stresses of the dislocation stress field, it can be derived that (Zhang et al., 1999)

$$\begin{aligned} &E_{\mathrm{s}} = E_0 + E_{\mathrm{c}}, \quad E_0 = -\frac{1}{2}\int_{r_0}^{L} \sigma_{a,ij} n_j b_i \,\mathrm{d}s, \\ &E_{\mathrm{c}} = \frac{1}{2}\oint_{c_{r_0}} \sigma_{a,ij} n_j u_{a,i} \,\mathrm{d}s, \quad E_{\mathrm{int}} = -\int_0^L \sigma_{m,ij} n_j b_i \,\mathrm{d}s, \end{aligned} \tag{2}$$

where σ is the stress, the subscripts, a and m, denote the dislocation and the mismatch, respectively. i and j can be either 1, 2, or 3 for the Cartesian coordinates, n_i is a unit vector normal to the integral contour, and L is the length of the cut.

The solution of the self-energy is contingent upon the determination of the elastic stress field, $\sigma_{a,ij}$, arising from the dislocation. However, due to the free surface condition at $x_2 = h$ and the difference in elastic constants between the film and the substrate, the derivation of the stress field is complex. Both the superposition principle (Suo and Hutchinson, 1990) and Fourier integral (Civelek, 1985) are adopted in the present study to derive the stress field. The stress field, $\sigma_{a,ij}$, due to the interface dislocation can be derived by superposition of the following two stress components: (1) σ^0_{ij}, the stress due to the interface dislocation assuming the film is also semi-infinite, and (2) σ^*_{ij}, the stress due to prescribed traction on the film surface which are the negative of those calculated from the first stress component at $x_2 = h$. That is

$$\sigma_{a,ij} = \sigma^0_{ij} + \sigma^*_{ij} \tag{3}$$

and the stress-free condition at $x_2 = h$ for $\sigma_{a,ij}$ is hence satisfied. The detailed derivations of σ^0_{ij} and σ^*_{ij} are given in Appendices A and B for an edge dislocation and a screw dislocation, respectively.

The mismatch stress and strain fields, σ and ε, in the film and substrate can be derived from the force balance condition, and the compatibility condition.

Considering a semi-infinite substrate and using Eq. (2), the mismatch strain energy can be obtained, such that

$$E_{\text{int}} = M\varepsilon_{\text{m}}^{0} b_1 h, \tag{4}$$

where $M = 2\mu(1+\nu)/(1-\nu)$ is the biaxial modulus, $\varepsilon_{\text{m}}^{0} = (a_{\text{s}} - a_{\text{f}})/a_{\text{f}}$ is the unrelaxed mismatch strain, and a_{s} and a_{f} are the stress-free lattice parameters of the substrate and the film, respectively.

The strain energy, E_0, obtained from Eq. (2) and the stress fields, σ_{ij}^{0} and σ_{ij}^{*}, shown in Appendices A and B with the assumption of the core radius much smaller than the film thickness is

$$\begin{aligned} E_0 = {} & \left[\frac{(1+\alpha)\left(b_1^2+b_2^2\right)}{\pi c_{\text{s}}(1-\beta^2)} + \frac{\mu_{\text{eff}} b_3^2}{4\pi}\right] \ln\left(\frac{h}{r_0}\right) + \frac{\mu_{\text{eff}} b_3^2}{4\pi}\left[\ln(2) + \sum_{n=1}^{\infty}\left(\frac{\mu_1-\mu_2}{\mu_1+\mu_2}\right)^n \ln\left(\frac{1+n}{n}\right)\right] \\ & + E_{0,e_1} + E_{0,e_2} + E_{0,e_3}, \end{aligned} \tag{5}$$

where

$$\begin{aligned} E_{0,e_1} = {} & -\frac{1+\alpha}{\pi c_{\text{s}}(1-\beta^2)} \sum_{n=0}^{\infty}\sum_{p=0}^{n} d_0^{*}\Bigg\{ -\frac{\left(B_{21}b_1^2 + A_{21}b_2^2\right)}{\gamma_1+1} + \frac{(B_{41}-B_{22})b_1^2 - (A_{41}+A_{22})b_2^2}{\gamma_1-1} \\ & + \frac{\left(B_{42}b_1^2 - A_{42}b_2^2\right)}{\gamma_1-3} + \ln(\gamma_1+1)\left[(B_{11}-B_{21})b_1^2 + A_{11}b_2^2\right] \\ & + \ln(\gamma_1)\left[(B_{21}+B_{31}+B_{41}-B_{11})b_1^2 - (A_{11}+A_{31})b_2^2\right] \\ & + \ln(\gamma_1-1)\left[(B_{12}-B_{22}-B_{31}-B_{41})b_1^2 + (A_{12}+A_{31})b_2^2\right] \\ & + \ln(\gamma_1-2)\left[(B_{22}+B_{32}+B_{42}-B_{12})b_1^2 - (A_{12}+A_{32})b_2^2\right] \\ & + \ln(\gamma_1-3)\left[A_{32}b_2^2 - (B_{32}+B_{42})b_1^2\right]\Bigg\}, \end{aligned} \tag{6a}$$

$$\begin{aligned} E_{0,e_2} = {} & -\frac{(1+\alpha)}{\pi c_{\text{s}}(1-\beta^2)} \sum_{n=1}^{\infty}\sum_{p=1}^{n}\sum_{q=1}^{p} d_0\Bigg\{(f-1)!\Bigg[\left\langle (B_{11}-2B_{21})b_1^2 - (A_{21}-A_{11})b_2^2\right\rangle \left\langle \frac{1}{\gamma_2^f} - \frac{1}{(\gamma_2+1)^f}\right\rangle \\ & + \left\langle (B_{12}-2B_{22})b_1^2 - (A_{22}-A_{12})b_2^2\right\rangle \left\langle \frac{1}{(\gamma_2-2)^f} - \frac{1}{(\gamma_2-1)^f}\right\rangle \\ & - \left\langle (B_{31}+2B_{41})b_1^2 - (A_{31}+A_{41})b_2^2\right\rangle \left\langle \frac{1}{\gamma_2^f} - \frac{1}{(\gamma_2-1)^f}\right\rangle \\ & - \left\langle (B_{32}+2B_{42})b_1^2 - (A_{32}+A_{42})b_2^2\right\rangle \left\langle \frac{1}{(\gamma_2-2)^f} - \frac{1}{(\gamma_2-3)^f}\right\rangle \\ & + \left(B_{21}b_1^2 + A_{21}b_2^2\right)\left\langle \frac{1}{\gamma_2^f} - \frac{f}{(\gamma_2+1)^{f+1}} - \frac{1}{(\gamma_2+1)^f}\right\rangle \\ & + \left(B_{41}b_1^2 - A_{41}b_2^2\right)\left\langle \frac{1}{\gamma_2^f} + \frac{f}{(\gamma_2-1)^{f+1}} - \frac{1}{(\gamma_2-1)^f}\right\rangle \end{aligned}$$

$$+\left(B_{22}b_1^2+A_{22}b_2^2\right)\left\langle\frac{1}{(\gamma_2-2)^f}-\frac{f}{(\gamma_2-1)^{f+1}}-\frac{1}{(\gamma_2-1)^f}\right\rangle$$
$$+\left(B_{42}b_1^2-A_{42}b_2^2\right)\left\langle\frac{1}{(\gamma_2-2)^f}+\frac{f}{(\gamma_2-3)^{f+1}}-\frac{1}{(\gamma_2-3)^f}\right\rangle\Bigg]\Bigg\}, \tag{6b}$$

$$\begin{aligned}E_{0,e_3}=&-\frac{(1+\alpha)}{\pi c_s(1-\beta^2)}\sum_{n=0}^{\infty}\sum_{p=0}^{n}\sum_{q=0}^{p}d_0\Bigg\{f!\Bigg[\left\langle(B_{13}-2B_{23})b_1^2-(A_{23}-A_{13})b_2^2\right\rangle\left\langle\frac{1}{(\gamma_2-2)^{f+1}}\right.\\&\left.-\frac{1}{(\gamma_2-1)^{f+1}}\right\rangle-\left\langle(B_{33}+2B_{43})b_1^2-(A_{33}+A_{43})b_2^2\right\rangle\left\langle\frac{1}{(\gamma_2-2)^{f+1}}-\frac{1}{(\gamma_2-3)^{f+1}}\right\rangle\\&+\left(B_{23}b_1^2+A_{23}b_2^2\right)\left\langle\frac{1}{(\gamma_2-2)^{f+1}}-\frac{f+1}{(\gamma_2-1)^{f+2}}-\frac{1}{(\gamma_2-1)^{f+1}}\right\rangle\\&+\left(B_{43}b_1^2-A_{43}b_2^2\right)\left\langle\frac{f+1}{(\gamma_2-3)^{f+2}}+\frac{1}{(\gamma_2-2)^{f+1}}-\frac{1}{(\gamma_2-3)^{f+1}}\right\rangle\Bigg]\\&+(f+1)!\Bigg[\left\langle(B_{14}-2B_{24})b_1^2-(A_{24}-A_{14})b_2^2\right\rangle\left\langle\frac{1}{(\gamma_2-2)^{f+2}}-\frac{1}{(\gamma_2-1)^{f+2}}\right\rangle\\&-\left(B_{34}b_1^2-A_{34}b_2^2\right)\left\langle\frac{1}{(\gamma_2-2)^{f+2}}-\frac{1}{(\gamma_2-3)^{f+2}}\right\rangle\\&+\left(B_{24}b_1^2+A_{24}b_2^2\right)\left\langle\frac{1}{(\gamma_2-2)^{f+2}}-\frac{f+2}{(\gamma_2-1)^{f+3}}-\frac{1}{(\gamma_2-1)^{f+2}}\right\rangle\Bigg]\Bigg\},\end{aligned} \tag{6c}$$

$$k_f=3-4\nu_f,\quad k_s=3-4\nu_s, \tag{6d}$$

$$\alpha=\frac{\mu_f(k_s+1)-\mu_s(k_f+1)}{\mu_f(k_s+1)+\mu_s(k_f+1)},\quad \beta=\frac{\mu_f(k_s-1)-\mu_s(k_f-1)}{\mu_f(k_s+1)+\mu_s(k_f+1)}, \tag{6e}$$

$$\mu_{\text{eff}}=2\mu_s\mu_f/(\mu_s+\mu_f), \tag{6f}$$

$$d_0^*=\frac{2^{n-p}n!}{p!(n-p)!}\frac{d_2^{n-p}d_4^p}{d_1^{n+1}}, \tag{6g}$$

$$d_0=\frac{2^{n-p+2q}n!}{q!(p-q)!(n-p)!}\frac{d_2^{n-p}d_3^qd_4^{p-q}}{d_1^{n+1}}, \tag{6h}$$

$$d_1=(\mu_f-\mu_s)^2+\mu_f\mu_s(\mu_f-\mu_s)(c_f-c_s)-\mu_f^2\mu_s^2c_fc_s, \tag{6i}$$

$$d_2=(\mu_f-\mu_s)^2+\mu_f\mu_s(\mu_f-\mu_s)(c_f-c_s)+\frac{1}{2}\mu_f^2\mu_s^2c_f(c_f-c_s), \tag{6j}$$

$$d_3 = (\mu_f - \mu_s)^2 - \mu_f\mu_s(\mu_f - \mu_s)c_s, \tag{6k}$$

$$d_4 = -(\mu_f - \mu_s)^2 - \mu_f\mu_s(\mu_f - \mu_s)(c_f - c_s), \tag{6l}$$

$$f = 2q, \tag{6m}$$

$$\gamma_1 = 2(n + p + 2), \quad \gamma_2 = 2(n + p - q + 2), \tag{6n}$$

$$c_f = (k_f + 1)/\mu_f, \quad c_s = (k_s + 1)/\mu_s. \tag{6o}$$

The first term in Eq. (5) arises from the stress field, σ^0_{ij}, of the dislocation. The second term in Eq. (5) corresponds to the stress field, σ^*_{ij}, of the screw component of dislocation calculated via the Fourier integral (see Appendix B). The last three terms in Eq. (5) are induced by the stress field, σ^*_{ij}, of the edge component of dislocation calculated via the Fourier integral (see Appendix A for details). It can be seen from Eqs. (5), (6a)–(6o) that only the first term be related to the film thickness.

When the cut is along the x_2-axis, strain energy, E_c, due to the core traction derived from Eq. (2) is (see Appendix C)

$$E_c = -\frac{1}{4\pi c_f^2}\left\{2(b_1^2 + b_2^2)\left[\frac{(1+\Lambda_1)^2}{\mu_f} - \frac{(1+\Lambda_2)^2}{\mu_s}\right] + (b_1^2 - b_2^2)\left[\frac{(1+\Lambda_1)}{\mu_f}\langle(k_f - 1)\Lambda_1 + 2\Lambda_2 - 3 - 3k_f\rangle \right.\right.$$
$$\left.\left. + \frac{(1+\Lambda_2)}{\mu_s}\langle 2\Lambda_1 + (k_s - 1)\Lambda_2 + 1 + k_s\rangle\right]\right\}, \tag{7}$$

where

$$\Lambda_1 = \frac{\mu_s - \mu_f}{\mu_f + k_f\mu_s}, \quad \Lambda_2 = \frac{\mu_s k_f - \mu_f k_s}{\mu_s + \mu_f k_s}. \tag{8}$$

Combining Eqs. (4), (5) and (7), the formation energy, E_f, for the isolated interface dislocation can be obtained. The critical thickness, h_0, of the film for the interface dislocation to form can be derived from zero formation energy, such that

$$\frac{(b_1^2 + b_2^2)(1+\alpha)}{\pi c_s(1-\beta^2)}\ln\left(\frac{h_0}{r_0}\right) + \frac{\mu_{eff} b_3^2}{4\pi}\left[\ln\left(\frac{2h_0}{r_0}\right) + \sum_{n=1}^{\infty}\left(\frac{\mu_f - \mu_s}{\mu_f + \mu_s}\right)^n \ln\left(\frac{1+n}{n}\right)\right]$$
$$- \frac{1}{4\pi c_f^2}\left\{2(b_1^2 + b_2^2)\left[\frac{(1+\Lambda_1)^2}{\mu_f} - \frac{(1+\Lambda_2)^2}{\mu_s}\right]\right.$$
$$\left. + (b_1^2 - b_2^2)\left[\frac{(1+\Lambda_1)}{\mu_f}\langle(k_f - 1)\Lambda_1 + 2\Lambda_2 - 3 - 3k_f\rangle + \frac{(1+\Lambda_2)}{\mu_s}\langle 2\Lambda_1 + (k_s - 1)\Lambda_2 + 1 + k_s\rangle\right]\right\}$$
$$+ E_{0,e_1} + E_{0,e_2} + E_{0,e_3} = \frac{2\mu_f(1+\nu_f)}{1-\nu_f}\left|\epsilon^0_m b_1\right| h_0. \tag{9}$$

When the film and the substrate have the same elastic constants, Eq. (9) can be reduced to

$$\frac{\mu_f}{4\pi(1-\nu_f)}\left[b_1^2 + b_2^2 + (1-\nu_f)b_3^2\right]\ln\left(\frac{2h_0}{r_0}\right) - \frac{\mu_f b_2^2}{4\pi(1-\nu_f)} = \frac{2\mu_f(1+\nu_f)}{1-\nu_f}\left|\epsilon^0_m b_1\right| h_0. \tag{10}$$

Furthermore, when the core energy, $E_c = \mu_f(b_1^2 - b_2^2)/8\pi(1 - \nu_f)$, is ignored, Eq. (10) becomes the same as that obtained in the literature (Freund, 1993; Zhang, 1996; Zhang et al., 1999).

3. Results

In order to verify the free-surface condition and the continuity condition at the interface, the contours of predicted stress fields near an edge dislocation and a screw dislocation located at the origin on the interface (see Fig. 1) are shown, respectively. The predicted critical film thickness for the interface dislocation to form is then presented and compared with that from Zhang's analysis (Zhang, 1995).

3.1. Stress fields

To plot the stress fields, $\mu_s = 2\mu_f$, $\nu_f = 0.25$, and $\nu_s = 0.3$ are used in the present study to elucidate the essential trend. The contours of stress fields σ_{22} and σ_{12} arising from an edge dislocation with Burgers vector along the x_1 direction are plotted in Figs. 2(a) and (b), respectively. It can be seen from Figs. 2(a) and (b) that σ_{22} and σ_{12} are traction-free at the free surface $x_2 = h$ and continuous at the interface $x_2 = 0$. The stress fields, σ_{22} and σ_{12} are symmetric and anti-symmetric with respect to x_1, respectively. For the same stress level, the size of σ_{12} contour is greater in the film than in the substrate because the film is softer than the substrate.

The contours of stress fields σ_{22} and σ_{12} produced by an edge dislocation with a Burgers vector along the x_2 direction are plotted in Figs. 3(a) and (b), respectively. Again, σ_{22} and σ_{12} satisfy the traction-free condition at the free surface and the continuity condition at the interface. The stress fields, σ_{22} and σ_{12}, are anti-symmetric and symmetric with respect to x_1, respectively. In addition to contours passing the origin, two sets of symmetric close contours appear in the upper left and upper right regions for stress field, σ_{12}.

The stress field σ_{23} resulting from a screw dislocation with its Burgers vector along the x_3 direction is shown in Fig. 4. It can be seen from Fig. 4 that σ_{23} is zero at $x_2 = h$ and is continuous at $x_2 = 0$. The stress field, σ_{23}, is anti-symmetric with respect to x_1. The contours are more closely spaced in the film than in the substrate.

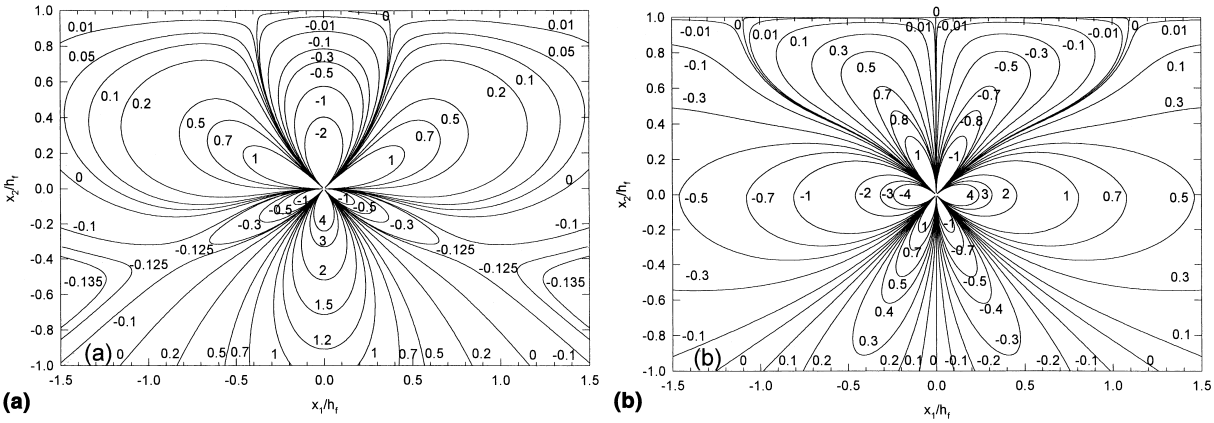

Fig. 2. The stress contours of an edge dislocation with a Burgers vector $\mathbf{b}_1$ along the x_1 direction showing (a) σ_{22} and (b) σ_{12}. The unit of stress is $2(1+\alpha)b_1/\pi c_s(1-\beta^2)h$.

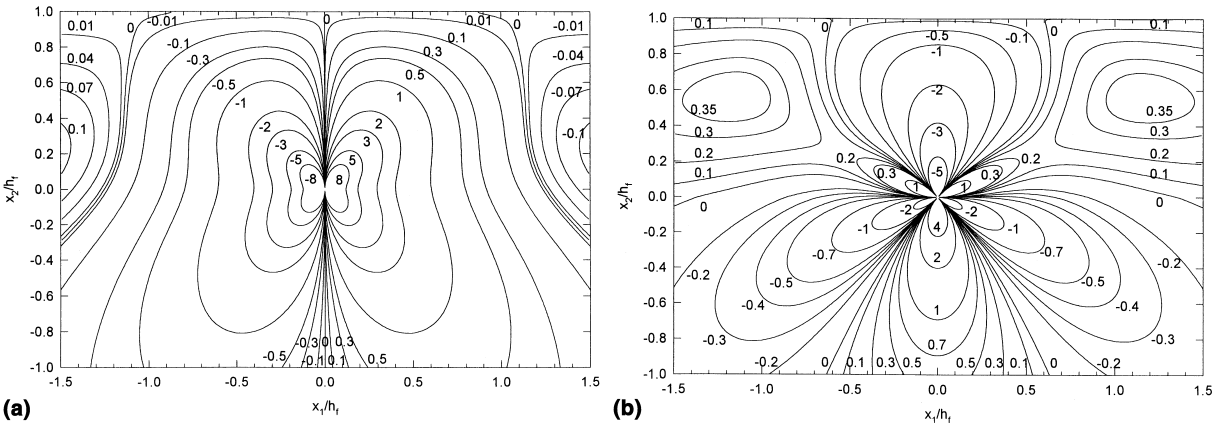

Fig. 3. The stress contours of an edge dislocation with a Burgers vector $\mathbf{b}_2$ along the x_2 direction showing (a) σ_{22} and (b) σ_{12}. The unit of stress is $2(1+\alpha)b_2/\pi c_s(1-\beta^2)h$.

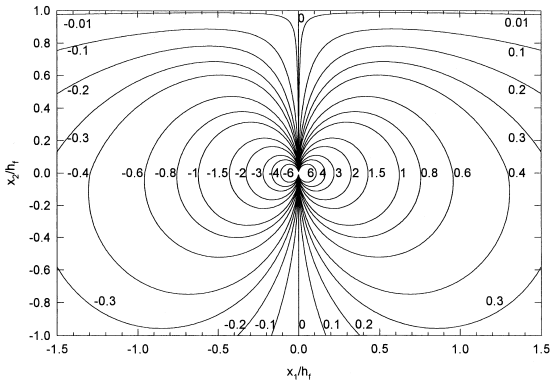

Fig. 4. The stress contours of a screw dislocation with a Burgers vector $\mathbf{b}_3$ along the x_3 direction showing σ_{23}. The unit of stress is $\mu_f b_3/2\pi h$.

3.2. The critical film thickness and comparison

The crystal structure of most semiconductor materials is diamond or zincblende. The principal types of dislocations in the strong Peierls potential of semiconductor crystals are the 60° dislocation and the screw dislocation lying in the $\langle 1\,1\,0\rangle$ direction (Alexander, 1986). Because the screw dislocation does not contribute to the mismatch stress, the pure screw dislocation is not considered in the present study. Instead, the 60° dislocation lying in the $\{1\,1\,1\}$ plane is analyzed, and a possible Burgers vector is $\mathbf{b} = b[0, 1/\sqrt{2}, 1/\sqrt{2}]$. Assume that a dislocation of Burgers vector $\mathbf{b} = b[1/2, \overline{1}/\sqrt{2}, 1/2]$ is located at the origin of interface as shown in Fig. 1, where x_1, x_2 and x_3 are in the $[1\,1\,0]$, $[0\,0\,1]$ and $[\overline{1}\,1\,0]$ directions, respectively. Using Eq. (9), and $\nu_f = \nu_s = 0.25$ and $r_0 = 0.25b$, the critical thickness of the film, h_0, to form a dislocation as a function of the shear modulus ratio, μ_f/μ_s, is plotted as the solid line in Fig. 5 at different magnitudes of mismatch strain, $|\varepsilon_m^0|$. It is found that the critical thickness decreases monotonically with increasing shear modulus ratio of the film to the substrate, μ_f/μ_s, and mismatch strain. The results from Zhang's analysis are also shown (see the dashed line in Fig. 5). Comparing to Zhang's results (Zhang, 1995), the present results predict a smaller critical film thickness; however, the difference decreases with increasing shear modulus ratio, μ_f/μ_s.

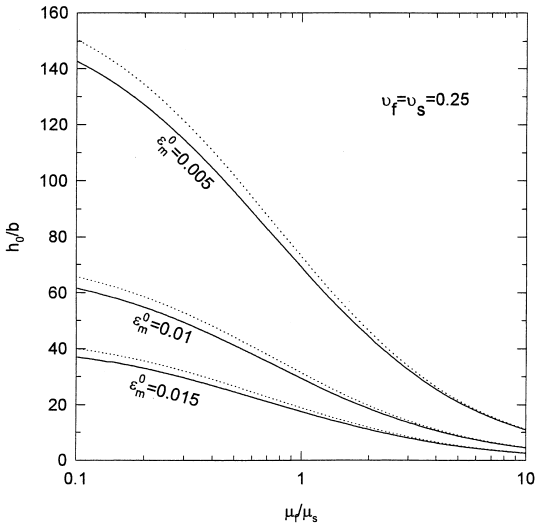

Fig. 5. The critical thickness as a function of shear modulus with parameter ε_m^0.

4. Conclusions

The effect of substrate modulus difference on dislocation formation in an epitaxial film is analyzed in the present study. The energy approach is used to study the critical film thickness for the interface dislocation to form. The self-energy of the dislocation and the interaction energy between the dislocation and the mismatch strain are calculated. However, in order to calculate these energies, the elastic stress fields resulting from an interface dislocation (i.e., $\sigma_{a,ij}$) and from the lattice mismatch between the film and the substrate (i.e., $\sigma_{m,ij}$) are required. Whereas $\sigma_{m,ij}$ can be readily derived from the force balance condition, the derivation of $\sigma_{a,ij}$ is complicated by both the free surface condition at the film surface and the difference in elastic constants between the film and the substrate. Both the superposition principle and Fourier integral are adopted in the present study to derive $\sigma_{a,ij}$. The elastic stress field, $\sigma_{a,ij}$, can be obtained by superposition of the elastic stress fields of the film/substrate system with the following two configurations: (i) a dislocation at the interface assuming the film is also semi-infinite, and (ii) prescribed traction on the film surface which are the negative of those calculated from the first configuration at the location equivalent to the film surface in the second configuration.

The elastic stress fields in the film/substrate system with an edge dislocation (Figs. 2 and 3) and a screw dislocation (Fig. 4) at the interface are analyzed, respectively. The predicted stress contours satisfy both the free-surface condition at the film surface and the continuity condition at the interface. The critical thickness of an epitaxial film to form a dislocation at the interface is calculated (Fig. 5). The results show that for a given shear modulus ratio of the film to the substrate (i.e., μ_f/μ_s), the critical film thickness decreases with increasing mismatch strain magnitude and core radius. For a given mismatch strain, the critical film thickness decreases with increasing μ_f/μ_s.

Acknowledgements

This work was financially supported by the National Science Council, Taiwan (SL), and the US Department of Energy, Division of Materials Science, Office of Basic Energy Sciences, under contract DE-AC05-96OR22464 with Lockheed Martin Energy Research Corp. (CHH).

Appendix A. The stress field, $\sigma_{a,ij}$, due to an edge dislocation at the interface

For an isotropically elastic problem, in-plane and anti-plane elastic deformation can be solved separately. An edge dislocation of Burgers vector $[b_1, b_2, 0]$ is located at the perfectly bonded interface between an epitaxial film of thickness h and a semi-infinite substrate as shown in Fig. 1. This problem can be solved by superposition of (1) a dislocation at the film/substrate interface assuming the film is also semi-infinite and (2) the actual film/substrate system without dislocations but with traction prescribed along the film surface as the negative of those calculated along $x_2 = h$ in case (1). Combination of the stress fields from the above two cases results in a traction-free surface at $x_2 = h$.

The case (1) has been solved by Suo and Hutchinson (1989), such that

$$\begin{aligned}\sigma_{22}^0 + \mathrm{i}\sigma_{12}^0 &= \overline{B}\left[\frac{2x_1}{\rho^2} + \mathrm{i}\frac{2\beta^* x_2}{\rho^2}\right] + B(1+\beta^*)\left[\frac{4x_1x_2^2}{\rho^4} + \mathrm{i}\left(\frac{2x_2}{\rho^2} - \frac{4x_2^3}{\rho^4}\right)\right] \quad \text{for } x_2 \neq 0 \\ &= \overline{B}\left[\frac{2}{x_1} + \mathrm{i}2\pi\beta\delta(x_1)\right] \quad \text{for } x_2 = 0,\end{aligned} \tag{A.1a}$$

$$\sigma_{11}^0 + \sigma_{22}^0 = \frac{2(1+\beta^*)}{\rho^2}\left[B(x_1 - \mathrm{i}x_2) + \overline{B}(x_1 + \mathrm{i}x_2)\right], \tag{A.1b}$$

where

$$\rho^2 = x_1^2 + x_2^2, \tag{A.2a}$$

$$B = \frac{(1+\alpha)(b_1 + \mathrm{i}b_2)}{\mathrm{i}\pi c_s(1-\beta^2)}, \tag{A.2b}$$

$$\begin{aligned}\beta^* &= \beta \quad \text{for } x_2 > 0, \\ \beta^* &= -\beta \quad \text{for } x_2 < 0,\end{aligned} \tag{A.2c}$$

where α and c_s are defined by Eqs. (6e) and (6o), and δ is the Dirac delta function.

The solutions for case (2) can be obtained using the Fourier transform method (Civelek, 1985). Two potentials, $U(x_1, x_2)$ and $\chi(x_1, x_2)$, are used which satisfy:

$$\Delta^2 U = 0, \quad \Delta\chi = 0, \quad \frac{\partial^2\chi}{\partial x_1 \partial x_2} = \frac{1}{4}\Delta U, \tag{A.2c}$$

where $\Delta = \partial^2/\partial x_1^2 + \partial^2/\partial x_2^2$. The stresses and the displacements can be obtained from $U(x_1, x_2)$ and $\chi(x_1, x_2)$, such that

$$\sigma_{11}^* = \frac{\partial^2 U}{\partial x_2^2}, \quad \sigma_{22}^* = \frac{\partial^2 U}{\partial x_1^2}, \quad \sigma_{12}^* = \frac{-\partial^2 U}{\partial x_1 \partial x_2}, \tag{A.4a}$$

$$2\mu u_1^* = -\frac{\partial U}{\partial x_1} + (k+1)\frac{\partial\chi}{\partial x_2}, \quad 2\mu u_2 = -\frac{\partial U}{\partial x_2} + (k+1)\frac{\partial\chi}{\partial x_1}, \tag{A.4b}$$

where k is expressed in Eq. (6d). The solutions of stresses and displacements from Eq. (A.4a) and (A.4b) are contingent upon the solutions of the two potentials, $U(x_1, x_2)$ and $\chi(x_1, x_2)$.

It is noted that the solution of $U(x_1, x_2)$ can be separated into two parts: one is symmetric and the other is antisymmetric in changing x_1 to $-x_1$. The stress field due to an edge dislocation with a Burgers vector b_1 along the x_1 direction is an example resulting from $U(x_1, x_2)$ of the symmetric part. In this case, the two potentials can be represented by Fourier integrals, such that

$$U_1 = \int_0^\infty \left\{ \left(\frac{B_1}{\omega^2} + \frac{B_2}{\omega} x_2 \right) \mathrm{e}^{-\omega x_2} + \left(\frac{B_3}{\omega^2} + \frac{B_4}{\omega} x_2 \right) \mathrm{e}^{\omega x_2} \right\} \cos(\omega x_1)\, \mathrm{d}\omega, \tag{A.5a}$$

$$\chi_1 = \int_0^\infty \frac{1}{2\omega^2} (B_2 \mathrm{e}^{-\omega x_2} + B_4 \mathrm{e}^{\omega x_2}) \sin(\omega x_1)\, \mathrm{d}\omega \tag{A.5b}$$

for $h \geqslant x_2 \geqslant 0$ and

$$U_2 = \int_0^\infty \left(\frac{B_5}{\omega^2} + \frac{B_6}{\omega} x_2 \right) \mathrm{e}^{\omega x_2} \cos(\omega x_1)\, \mathrm{d}\omega, \tag{A.5c}$$

$$\chi_2 = \int_0^\infty \frac{B_6}{2\omega^2} \mathrm{e}^{\omega x_2} \sin(\omega x_1)\, \mathrm{d}\omega \tag{A.5d}$$

for $x_2 \leqslant 0$ where the coefficients, B_i $(i = 1, 2, 3, 4, 5, 6)$, are determined by the boundary conditions. Using the traction-free condition at the free surface and the continuity conditions for the stress, σ_{12} and σ_{22}, and the displacements, u_1 and u_2, at the interface, solutions of B_i $(i = 1, 2, 3, 4, 5, 6)$ are:

$$B_i = \frac{2\mathrm{i}\lambda_1}{D} \left\{ B_{i1} + \left(B_{i2} + h\omega B_{i3} + h^2\omega^2 B_{i4} \right) \mathrm{e}^{2h\omega} \right\}, \tag{A.6a}$$

$$D = d_1 \mathrm{e}^{4h\omega} - (2d_2 + 4d_3\omega^2 h^2) \mathrm{e}^{2h\omega} - d_4, \tag{A.6b}$$

where

$$\mathrm{i}\lambda_1 = \frac{(1+\alpha) b_1}{\pi c_\mathrm{s} \left(1 - \beta^2\right)}, \tag{A.7}$$

$$B_{11} = -\beta(\mu_\mathrm{f} - \mu_\mathrm{s})[\mu_\mathrm{f} - \mu_\mathrm{s} + (c_\mathrm{f} - c_\mathrm{s})\mu_\mathrm{f}\mu_\mathrm{s}], \tag{A.8a}$$

$$B_{12} = -(1-\beta) c_\mathrm{f} \mu_\mathrm{f} \mu_\mathrm{s} \left[\mu_\mathrm{f} - \mu_\mathrm{s} + \frac{(c_\mathrm{f} - c_\mathrm{s})}{2} \mu_\mathrm{f} \mu_\mathrm{s} \right] + \beta(\mu_\mathrm{f} - \mu_\mathrm{s})(\mu_\mathrm{f} - \mu_\mathrm{s} - c_\mathrm{s}\mu_\mathrm{f}\mu_\mathrm{s}), \tag{A.8b}$$

$$B_{13} = (1+\beta) c_\mathrm{f} \mu_\mathrm{f} \mu_\mathrm{s} [2(\mu_\mathrm{f} - \mu_\mathrm{s}) + (c_\mathrm{f} - c_\mathrm{s})\mu_\mathrm{f}\mu_\mathrm{s}] + 2\beta(\mu_\mathrm{f} - \mu_\mathrm{s})(\mu_\mathrm{f} - \mu_\mathrm{s} - c_\mathrm{s}\mu_\mathrm{f}\mu_\mathrm{s}), \tag{A.8c}$$

$$B_{14} = 2(1+\beta)(\mu_\mathrm{f} - \mu_\mathrm{s})(\mu_\mathrm{f} - \mu_\mathrm{s} - c_\mathrm{s}\mu_\mathrm{f}\mu_\mathrm{s}), \tag{A.8d}$$

$$B_{21} = -(1+\beta)(\mu_\mathrm{f} - \mu_\mathrm{s})[\mu_\mathrm{f} - \mu_\mathrm{s} + (c_\mathrm{f} - c_\mathrm{s})\mu_\mathrm{f}\mu_\mathrm{s}], \tag{A.8e}$$

$$2B_{22} = -\frac{1+\beta}{1-\beta} B_{23} = \frac{B_{24}}{2} = \frac{2(1+\beta)}{1-\beta} B_{41} = B_{14}, \tag{A.8f}$$

$$B_{31} = B_{13}/2, \tag{A.8g}$$

$$B_{32} = -\beta(\mu_\mathrm{f} - \mu_\mathrm{s} + c_\mathrm{f}\mu_\mathrm{f}\mu_\mathrm{s})(\mu_\mathrm{f} - \mu_\mathrm{s} - c_\mathrm{s}\mu_\mathrm{f}\mu_\mathrm{s}), \tag{A.8h}$$

$$B_{33} = 2B_{32} = \frac{\beta}{1+\beta} B_{34} = \frac{2\beta}{1-\beta} B_{42} = \frac{-\beta}{1+\beta} B_{43}, \tag{A.8i}$$

$$B_{44} = B_{64} = 0, \tag{A.8j}$$

$$B_{51} = \frac{c_f \mu_f \mu_s}{2}[2(\mu_f - \mu_s) + (1+\beta)(c_f - c_s)\mu_f \mu_s], \tag{A.8k}$$

$$B_{52} = \frac{c_f \mu_f \mu_s}{2}[-2(\mu_f - \mu_s) - (c_f - c_s)\mu_f \mu_s + \beta \mu_f \mu_s (c_f + c_s)], \tag{A.8l}$$

$$B_{53} = c_f \mu_f \mu_s [2(\mu_f - \mu_s) + (1+\beta) c_f \mu_f \mu_s - (1-\beta) c_s \mu_f \mu_s], \tag{A.8m}$$

$$B_{54} = -2(1+\beta) c_f \mu_f \mu_s (\mu_f - \mu_s - c_s \mu_f \mu_s), \tag{A.8n}$$

$$B_{61} = -(1-\beta) c_f \mu_f \mu_s (\mu_f - \mu_s), \tag{A.8o}$$

$$B_{62} = (1-\beta) c_f \mu_f \mu_s (\mu_f - \mu_s + c_f \mu_f \mu_s), \tag{A.8p}$$

$$B_{63} = -\frac{2(1+\beta)}{1-\beta} B_{62}. \tag{A.8q}$$

The stress field due to an edge dislocation with a Burgers vector $\mathbf{b}_2$ along the x_2 direction is an example resulting from $U(x_1, x_2)$ of the antisymmetric part. In this case, the two potentials used are:

$$U_3 = \int_0^\infty \left\{ \left(\frac{A_1}{\omega^2} + \frac{A_2 x_2}{\omega} \right) e^{-\omega x_2} + \left(\frac{A_3}{\omega^2} + \frac{A_4 x_2}{\omega} \right) e^{\omega x_2} \right\} \sin(\omega x_1)\, d\omega, \tag{A.9a}$$

$$\chi_3 = \int_0^\infty -\frac{1}{2\omega^2} (A_2 e^{-\omega x_2} + A_4 e^{\omega x_2}) \cos(\omega x_1)\, d\omega \tag{A.9b}$$

for $h \geqslant x_2 \geqslant 0$ and

$$U_4 = \int_0^\infty \left(\frac{A_5}{\omega^2} + \frac{A_6}{\omega} x_2 \right) e^{\omega x_2} \sin(\omega x_1)\, d\omega \tag{A.9c}$$

$$\chi_4 = -\frac{1}{2} \int_0^\infty \frac{A_6}{\omega^2} e^{\omega x_2} \cos(\omega x_1)\, d\omega \tag{A.9d}$$

for $x_2 \leqslant 0$. Using the traction-free conditions at the free surface and the continuity conditions at the interface, solutions of A_i $(i = 1, 2, 3, 4, 5, 6)$ are

$$A_i = \frac{2\lambda_2}{D} \left\{ A_{i1} + \left(A_{i2} + h\omega A_{i3} + h^2 \omega^2 A_{i4} \right) e^{2h\omega} \right\}, \tag{A.10}$$

where

$$\lambda_2 = \frac{(1+\alpha) b_2}{\pi c_s (1-\beta^2)}, \tag{A.11}$$

$$A_{11} = A_{21}/(1+\beta) = -B_{11}/\beta, \tag{A.12a}$$

$$A_{12} = -(\mu_f - \mu_s)^2 - (c_f - c_s)\mu_f\mu_s(\mu_f - \mu_s) - \frac{(1-\beta)}{2}c_f(c_f - c_s)\mu_f^2\mu_s^2 + \beta c_f\mu_f\mu_s(\mu_f - \mu_s), \tag{A.12b}$$

$$A_{13} = -2(\mu_f - \mu_s)^2 - 2(c_f - c_s)\mu_f\mu_s(\mu_f - \mu_s) - (1+\beta)c_f(c_f - c_s)\mu_f^2\mu_s^2 - 2\beta c_f\mu_f\mu_s(\mu_f - \mu_s), \tag{A.12c}$$

$$A_{14} = -2(1+\beta)(\mu_f - \mu_s)^2 + 2(1+\beta)c_s\mu_f\mu_s(\mu_f - \mu_s), \tag{A.12d}$$

$$2A_{22} = \frac{1+\beta}{1-\beta}A_{23} = \frac{A_{24}}{2} = -\frac{2(1+\beta)}{(1-\beta)}A_{41} = A_{14}, \tag{A.12e}$$

$$A_{31} = A_{13}/2, \tag{A.12f}$$

$$A_{32} = A_{11} - c_f c_s \mu_f^2\mu_s^2, \tag{A.12g}$$

$$\frac{A_{33}}{2} = \frac{A_{34}}{2(1+\beta)} = \frac{A_{42}}{\beta - 1} = -\frac{A_{43}}{2(1+\beta)} = A_{32}, \tag{A.12h}$$

$$A_{44} = A_{64} = 0, \tag{A.12i}$$

$$A_{51} = -\beta c_f\mu_f\mu_s(\mu_f - \mu_s) - \frac{1+\beta}{2}c_f(c_f - c_s)\mu_f^2\mu_s^2, \tag{A.12j}$$

$$A_{52} = \beta c_f\mu_f\mu_s(\mu_f - \mu_s) + \frac{\beta}{2}c_f(c_f - c_s)\mu_f^2\mu_s^2 - \frac{c_f}{2}(c_f + c_s)\mu_f^2\mu_s^2, \tag{A.12k}$$

$$A_{53} = -2\beta c_f\mu_f\mu_s(\mu_f - \mu_s) - c_f(c_f + c_s)\mu_f^2\mu_s^2 - \beta c_f(c_f - c_s)\mu_f^2\mu_s^2, \tag{A.12l}$$

$$A_{54} = 2(1+\beta)\left[c_f\mu_f\mu_s(\mu_f - \mu_s) - c_f c_s\mu_f^2\mu_s^2\right], \tag{A.12m}$$

$$A_{61} = (\beta - 1)c_f\mu_f\mu_s(\mu_f - \mu_s), \tag{A.12n}$$

$$A_{62} = (1-\beta)\left[c_f\mu_f\mu_s(\mu_f - \mu_s) + c_f^2\mu_f^2\mu_s^2\right], \tag{A.12o}$$

$$A_{63} = \frac{2(1+\beta)}{(1-\beta)}A_{62}. \tag{A.12p}$$

The stress field, σ^*_{ij}, can be obtained by combining Eqs. (A.4a),(A.5a)–(A.5d), (A.8a)–(A.8q), (A.9a)–(A.9d), (A.12a)–(A.12p).

Appendix B. The stress field, $\sigma_{a,ij}$, due to a screw dislocation at the interface

A screw dislocation of Burgers vector $(0\ 0\ b_3)$ located at the perfectly bounded interface of the film/substrate system is considered. The procedure for analyzing the elastic stress field is similar to that of an edge dislocation. Alternatively, the solutions can also be obtained by reducing Chou's solutions (Chou,

1966), in which a screw dislocation in a three-phase medium is considered. Hence, without listing the derivation procedures, the stress components, σ^*_{23} and σ^*_{13}, are summarized as follows:

$$\sigma^*_{23} = \frac{\mu_{\text{eff}} b_3 x_1}{2\pi} \sum_{n=1}^{\infty} \left[\frac{\mu_{\text{fs}}^n}{x_1^2 + (x_2 + 2nh)^2} - \frac{\mu_{\text{fs}}^{n-1}}{x_1^2 + (x_2 - 2nh)^2} \right], \tag{B.1a}$$

$$\sigma^*_{13} = \frac{\mu_{\text{eff}} b_3}{2\pi} \sum_{n=1}^{\infty} \left[\frac{\mu_{\text{fs}}^{n-1}(x_2 - 2nh)}{x_1^2 + (x_2 - 2nh)^2} - \frac{\mu_{\text{fs}}^{n}(x_2 + 2nh)}{x_1^2 + (x_2 + 2nh)^2} \right] \tag{B.1b}$$

for $h \geqslant x_2 \geqslant 0$, and

$$\sigma^*_{23} = -\frac{\mu_{\text{eff}}^2 b_3 x_1}{2\pi\mu_{\text{f}}} \left\{ \sum_{n=1}^{\infty} \frac{\mu_{\text{fs}}^{n-1}}{x_1^2 + (x_2 - 2nh)^2} \right\}, \tag{B.1c}$$

$$\sigma^*_{13} = \frac{\mu_{\text{eff}}^2 b_3}{2\pi\mu_{\text{f}}} \sum_{n=1}^{\infty} \frac{\mu_{\text{fs}}^{n-1}(x_2 - 2nh)}{x_1^2 + (x_2 - 2nh)^2} \tag{B.1d}$$

for $x_2 \leqslant 0$, where

$$\mu_{\text{fs}} = \frac{\mu_{\text{f}} - \mu_{\text{s}}}{\mu_{\text{f}} + \mu_{\text{s}}}. \tag{B.1e}$$

Appendix C. The core energy

The stress and displacement fields due to two semi-infinite medium are used to calculate the core energy, E_{c}. The core energy in polar coordinate system is expressed as

$$E_{\text{c}} = \frac{1}{2} \oint \sigma^0_{ij} n_j u^0_i \, \mathrm{d}s = -\frac{1}{2} \int_{\theta_0}^{\theta_0 + 2\pi} \left(\sigma^0_{rr} u^0_r + \sigma^0_{r\theta} u^0_\theta + \sigma^0_{rz} u^0_z \right) r_0 \, \mathrm{d}\theta, \tag{C.1}$$

where θ_0 is the cutting angle. u^0_r, u^0_θ and σ^0_{rr}, $\sigma^0_{r\theta}$ are due to the edge component, and u^0_z and σ^0_{rz} are due to the screw component. Since σ^0_{rz} arising from the screw component is zero along the circle of dislocation core, only the edge component contributes to the core energy. Assume that the Burgers vector of edge component in complex form is

$$b_{\text{e}} = b_1 + \mathrm{i} b_2. \tag{C.2}$$

The stress and displacements arising from the edge component in the polar coordinate system are obtained from the Cartesian coordinate as

$$\sigma^0_{rr} - \mathrm{i}\sigma^0_{r\theta} = -\frac{\mathrm{i}2(1 + \Lambda_1) b_{\text{e}} \mathrm{e}^{-\mathrm{i}\theta}}{\pi c_{\text{f}} r_0} - \frac{\mathrm{i}(\Lambda_2 - \Lambda_1)\overline{b_{\text{e}}} \mathrm{e}^{\mathrm{i}\theta}}{\pi c_{\text{f}} r_0}, \tag{C.3a}$$

$$\begin{aligned} 2\pi(k_{\text{f}} + 1)(u_1 + \mathrm{i}u_2) = {} & \mathrm{i} \ln(r_0)[1 + \Lambda_2 - k_{\text{f}}(1 + \Lambda_1)] b_{\text{e}} + \theta b_{\text{e}}[1 + \Lambda_2 + (1 + \Lambda_1) k_{\text{f}}] \\ & + \mathrm{i}(1 + \Lambda_1)\overline{b_{\text{e}}}(1 - \mathrm{e}^{\mathrm{i}2\theta}) - 2\pi b_{\text{e}}(k_{\text{f}}\Lambda_1 + \Lambda_2) + \theta_0 b_{\text{e}}[\Lambda_2 - 1 + k_{\text{f}}(\Lambda_1 - 1)] \end{aligned} \tag{C.3b}$$

for $\theta_0 \leqslant \theta < \pi$,

$$\sigma_{rr}^0 - \mathrm{i}\sigma_{r\theta}^0 = -\frac{\mathrm{i}2(1+\Lambda_2)b_\mathrm{e}\mathrm{e}^{-\mathrm{i}\theta}}{\pi c_\mathrm{f} r_0} + \frac{\mathrm{i}(\Lambda_2-\Lambda_1)\overline{b_\mathrm{e}}\mathrm{e}^{\mathrm{i}\theta}}{\pi c_\mathrm{f} r_0}, \tag{C.3c}$$

$$\begin{aligned} 2\pi(1+k_\mathrm{f})(u_1+\mathrm{i}u_2) = \frac{\mu_\mathrm{f}}{\mu_\mathrm{s}}\big\{&\mathrm{i}\ln(r_0)b_\mathrm{e}[1+\Lambda_1-k_\mathrm{s}(1+\Lambda_2)] + (\theta-\theta_0)b_\mathrm{e}[1+\Lambda_2+(1+\Lambda_1)k_\mathrm{f}] \\ &+ \mathrm{i}\overline{b_\mathrm{e}}(1+\Lambda_2)(1-\mathrm{e}^{\mathrm{i}2\theta})\big\} \end{aligned} \tag{C.3d}$$

for $\pi \leqslant \theta < 2\pi$, and

$$\begin{aligned} 2\pi(k_\mathrm{f}+1)\big(u_1^0+\mathrm{i}u_2^0\big) = {}& \mathrm{i}\ln(r_0)b_\mathrm{e}[1+\Lambda_2-k_\mathrm{f}(1+\Lambda_1)] + \theta b_\mathrm{e}[1+\Lambda_2+(1+\Lambda_1)k_\mathrm{f}] \\ &+ \mathrm{i}(1+\Lambda_1)\overline{b_\mathrm{e}}(1-\mathrm{e}^{\mathrm{i}2\theta}) - 4\pi b_\mathrm{e}(k_\mathrm{f}\Lambda_1+\Lambda_2) + \theta_0 b_\mathrm{e}[\Lambda_2-1+k_\mathrm{f}(\Lambda_1-1)] \end{aligned} \tag{C.3e}$$

for $2\pi \leqslant \theta < 2\pi + \theta_0$. b_e is the complex conjugate of b_e. The expression of $(\sigma_{rr}^0 - \mathrm{i}\sigma_{r\theta}^0)$ in $2\pi \leqslant \theta < 2\pi + \theta_0$ is the same as that in $\theta_0 \leqslant \theta < \pi$ shown in Eq. (C.3a). The displacement in the polar coordinate system can be obtained from the Cartesian coordinate as

$$u_r^0 + \mathrm{i}u_\theta^0 = \big(u_1^0 + \mathrm{i}u_2^0\big)\mathrm{e}^{-\mathrm{i}\theta}. \tag{C.4}$$

Note that the displacement and stress are continuous at the interface and displacement jump is located at $\theta = \theta_0$. These conditions were not satisfied in Zhang's analysis (Zhang, 1995). After lengthy calculation, the core energy is

$$\begin{aligned} E_\mathrm{c} = {}& -\frac{1}{4\pi\mu_\mathrm{f}c_\mathrm{f}^2}\Bigg\{4(1+k_\mathrm{f})(1+\Lambda_1)b_1b_2\sin(2\theta_0) + (1+\Lambda_1)\big(b_1^2-b_2^2\big)[2(1+k_\mathrm{f})\cos 2\theta_0 + k_\mathrm{f}\Lambda_1 \\ &+ \Lambda_2 - k_\mathrm{f} - 1] - \frac{1}{4\pi c_\mathrm{f}^2}2\big(b_1^2+b_2^2\big)\left[\frac{(1+\Lambda_1)^2}{\mu_\mathrm{f}} - \frac{(1+\Lambda_2)^2}{\mu_\mathrm{s}}\right] \\ &+ \big(b_1^2-b_2^2\big)\frac{(1+\Lambda_2)}{\mu_\mathrm{s}}[k_\mathrm{s}(1+\Lambda_2)+1+\Lambda_1] + \big(b_1^2-b_2^2\big)(\Lambda_2-\Lambda_1)\left[\frac{1+\Lambda_1}{\mu_\mathrm{f}} - \frac{1+\Lambda_2}{\mu_\mathrm{s}}\right]\Bigg\}. \end{aligned} \tag{C.5}$$

If the cutting path is along $\theta_0 = \pi/2$, then Eq. (C.5) is reduced to Eq. (7).

References

Alexander, H., 1986. Dislocations in covalent crystals. In: Nabarro, F.R.N. (Ed.), Dislocations in Solids, vol. 7. Elsevier Science, Amsterdam, pp. 115–234.

Chou, Y.T., 1966. Screw dislocations in and near lamellar inclusions. Phys. Stat. Sol. 17, 509–516.

Civelek, M.B., 1985. Stress intensity factor for a system crack in an infinite strip. In: Kanninen M.F., Hopper, A.T. (Eds.), Fracture Mechanics: Sixteenth Symposium, ASTM STP 868. pp. 1–28.

Frank, F.C., Merwe, J.H., 1949. One dimensional dislocations: I. Static theory. Proc. R. Soc. Lond., A 198, 205–216.

Freund, L.B., 1990. The driving force for glide of a threading dislocation in a strained epitaxial layer on a substrate. J. Mech. Phys. Solids 38, 657–679.

Freund, L.B., 1993. The mechanics of dislocations in strained-layer semiconductor materials. Adv. Appl. Mech. 30, 1–66.

Freund, L.B., Nix, W.D., 1996. A critical thickness condition for a strained complaint substrate/epitaxial film system. Appl. Phys. Lett. 69, 173–175.

Gosling, T.J., Willis, J.R., 1994. The energy of an array of dislocations in an anisotropic half-space. Philos. Mag. A 69, 65–90.

Gutkin, M.Yu., Romanov, A.E., 1992. Screw dislocations in a thin-phase heteroepitaxial plate. Phys. Stat. Sol. 129, 117–126.

Mattews, J.W., Blakeslee, J.W., 1974. Defects in epitaxial multilayers. J. Cryst. Growth 27, 118–125.

Suo, Z., Hutchinson, J.W., 1989. Steady state cracking in brittle substrates beneath adherent films. Int. J. Solids Struct. 25, 1337–1353.
Suo, Z., Hutchinson, J.W., 1990. Interface crack between two elastic layers. Int. J. Fract. 43, 1–18.
Willis, J.R., Jain, S.C., Bullough, R., 1990. The energy of an array of dislocations: implications for strain relaxation in semiconductor heterostructures. Philos. Mag. A 62, 115–129.
Willis, J.R., Jain, S.C., Bullough, R., 1991. The energy of an array of dislocations: II. Consideration of a capped epitaxial layer. Philos. Mag. A 64, 629–640.
Zhang, T.Y., 1995. Effect of elastic constants on the critical thickness of an epilayer. Phys. Stat. Sol. (a) 152, 415–429.
Zhang, T.Y., 1996. Isotropic and anisotropic elasticity studies of mismatch dislocations, critical thickness and work hardening in epilayers. Defect and Diffusion Forum 136&137, 61–106.
Zhang, T.Y., Lee, S., Guido, L.J., Hsueh, C.H., 1999. Criteria for formation of interface dislocations in a finite thickness epilayer deposited on a substrate. J. Appl. Phys. 85, 7579–7586.